ICANS-XI International Collaboration on Advanced Neutron Sources
KEK, Tsukuba, October 22-26, 1990

Total Performance of Small-Angle Machines at Pulsed Source

M. Furusaka, N. Watanabe, K. Suzuya*, I. Fujikawa and S. Satoh
National Laboratory for High Energy Physics, Tsukuba 305, Japan
*Institute for Materials Research, Tohoku University, 2-1-1 Katahira, Sendai 980, Japan

Abstract

The total performance of a small-angle neutron-scattering (SANS) instrument is discussed in terms of the incident neutron intensity and solid angle covered by the detector system. Although the time-averaged neutron intensity is very low at a pulsed source compared with that at a reactor, there is a considerable gain in intensity for a SANS instrument at a pulsed source, even in the small-Q region when incident neutrons with a wide range of wavelengths are used together with a detector system covering a wide solid angle. A small/medium angle diffractometer, WINK, at KENS is described, which was designed so as to take full advantage of a wide incident-neutron spectrum and a nearly 4π-solid-angle detector.

Introduction

In terms of the "total performance", what parameters should be considered for a SANS instrument, especially one at a pulsed neutron source? Very often, in optimizing a SANS instrument, only the resolution and intensity relationship (in terms of incident neutron collimation and resolution of a detector system) has been discussed; the use of monochromatic neutrons has been implicitly assumed. In the case of a pulse source, it is essentially important to utilize neutrons of a wider range of wavelength, especially with smaller wave numbers, $k=|\mathbf{k}|$, together with a wide solid-angle detector system. There has been no established way for optimizing a collimator system used in a polychromatic neutron beam. In this paper, the optimization of a SANS instrument is discussed in terms of various parameters, such as the period of neutron bursts, the incident neutron intensity/spectrum and the solid angle covered by a detector system.

Intensity optimization

In the optimization of various parameters, one must first know the boundary conditions. From an experimental point of view, the relevant parameters are the required Q-range, especially a minimum Q (Q_{min}), Q-resolution ΔQ. In this paper all of the parameters are discussed (not in terms of wavelength (λ)) in the wave number (k).

One of the possible scenarios used in choosing a suitable collimation system from the required Q_{min} is shown in the following. From the fundamental equation, we can write,

$$Q = 2k_z \sin(\frac{\varphi}{2}) , \qquad (1)$$

where, k_z is the z-component of a wave number vector along the beam direction, and φ is the scattering angle. Then, dQ can be expressed as

$$dQ = 2 \sin\frac{\varphi}{2} dk_z + k_z \cos\frac{\varphi}{2} d\varphi . \qquad (2)$$

Usually, the angular uncertainty which is determined by the finite size of a sample and resolution elements of a detector system is sufficiently smaller than the incident beam collimation, i.e.,

$$(\Delta\varphi^f_{x,y})^2 \ll (\Delta\varphi^i_{x,y})^2 . \qquad (3)$$

Then, using $\Delta k_{x,y} = k_z \Delta\varphi_{x,y}$, ΔQ can be expressed to a convolution approximation,

$$\Delta Q = \left[(2 \sin\frac{\varphi}{2} \Delta k_z)^2 + (\cos\frac{\varphi}{2} k_z \Delta\varphi_x)^2 + (\cos\frac{\varphi}{2} k_z \Delta\varphi_y)^2 \right]^{1/2}$$
$$= \left[(2 \sin\frac{\varphi}{2} \Delta k_z)^2 + (\cos\frac{\varphi}{2} \Delta k_x)^2 + (\cos\frac{\varphi}{2} \Delta k_y)^2 \right]^{1/2} . \quad (4)$$

A relative resolution $R = \Delta Q/Q$ is expressed as

$$R = \frac{\Delta Q}{Q} = \left[(\frac{\Delta k_z}{k_z})^2 + (\frac{1}{2} \cot\frac{\varphi}{2} \Delta\varphi_x)^2 + (\frac{1}{2} \cot\frac{\varphi}{2} \Delta\varphi_y)^2 \right]^{1/2} . \quad (5)$$

In the case of a reactor, since k_z is constant, the first term is independent of Q. The second and the third terms are proportional to $\cot(\varphi/2)$, i.e. inversely proportional to Q at smaller angles.

In the case of a pulsed source, the following condition generally holds:

$$\varphi \Delta k_z \ll \Delta k_{x,y} . \quad (6)$$

Therefore, the first terms of eqs. (4) and (5) are negligible compared to the other terms.

ΔQ at Q_{min} (ΔQ_{min}) is determined by the required resolution, R, as $\Delta Q_{min} = Q_{min} \times R$ (typically $R \approx 0.1$). A suitable collimator system can be chosen according to ΔQ_{min}. If a relaxed resolution, R^* (say $R^* \approx 0.3$), can be acceptable at the lower angle part of the detector system, Q can be extended to $Q_{min}^* = Q_{min} \times R/R^*$ with the same incident collimator system.

The components in eq. (4) must be nearly equal from the condition of resolution matching. Using eq. (4) the required $\Delta k_{x,y}$ for ΔQ_{min} is expressed as

$$\Delta k_{x,y} \approx \frac{1}{\alpha} \Delta Q_{min} . \qquad \alpha = \begin{cases} \sqrt{2} : \text{pulsed source} \\ \sqrt{3} : \text{reactor} \end{cases} \quad (7)$$

The values of α can be easily understood from eq. (4). Using the smallest available kz (k_z^{min}), $\Delta\varphi_{x,y}$ is given by

$$\Delta\varphi_{x,y} = \frac{\Delta k_{x,y}}{k_z^{min}} = \frac{1}{\alpha} \frac{\Delta Q_{min}}{k_z^{min}} . \quad (8)$$

The neutron intensity at the sample position is discussed in terms of $\Delta\varphi_{x,y}$. When an isotopic sample is assumed, the neutron intensity observed in ΔQ at Q is expressed as

$$I^{obs}(Q) \Delta Q = \int_{k_z^{min}}^{k_z^{max}} dk_z \, I^0(k_z) \, \eta(k_z, Q) \, V \, N \, Att(k_z, Q) \frac{d\sigma}{d\Omega}(Q) \frac{\Delta\Omega(k_z, Q)}{\Delta Q} \Delta Q, \quad (9)$$

where, k_z^{max} is the largest k_z available, $I^0(k_z)$ the incident neutron intensity at the sample position, $\eta(k_z, Q)$ the detector efficiency, V the volume of a sample, N the number density, $Att(k_z, Q)$ the sample attenuation, $d\sigma/d\Omega$ the scattering cross section, and $\Delta\Omega(k_z, Q)/\Delta Q$ the solid-angle covered by the detector system in ΔQ for a fixed k_z. Since the V, N, $Att(k_z, Q)$ and $d\sigma/d\Omega$ in the integral are sample dependent, only the other factors are considered here. Our goal is to maximize the function F(Q) in the following form at a specified Q range:

$$F(Q) = \int_{k_z^{min}}^{k_z^{max}} dk_z \, I^0(k_z) \, \eta(k_z, Q) \frac{\Delta\Omega(k_z, Q)}{\Delta Q} . \quad (10)$$

$I^0(k_z)$ can be derived from the phase space density of neutrons at the moderator (Maier-Leibnitz, H. 1966). The phase space density is expressed as

$$\frac{\Delta^6 n}{\Delta V_p} = \frac{\Delta^6 n}{\Delta k_x \Delta k_y \Delta k_z \Delta x \Delta y \Delta z \cdot \hbar^6}, \tag{11}$$

where n is the number of neutrons in the phase-space volume, V_p; $k_{x,y,z}$ the x,y and z (beam direction) components of k; Δk_x, Δk_y and Δk_z the corresponding resolution elements; and Δx, Δy and Δz the resolution elements in real-space.

The intensity, $I(k_z)$, at the sample position through a unit area for given $\Delta k_x \Delta k_y \Delta k_z$ is expressed as (Alefeld B. and Kollmar A., 1985),

$$I(k_z)\,\Delta k_z = \frac{\phi k_z^3}{2\pi k_T^4} e^{-\frac{k_z^2}{k_T^2}} \cdot \Delta k_x \Delta k_y \Delta k_z, \tag{12}$$

with

$$k_T = \frac{\sqrt{2 m k_B T_N}}{\hbar}. \tag{13}$$

In the above ϕ is the time-averaged neutron flux of the Maxwellian part, m the neutron mass, k_B the Boltzman constant and T_N the effective neutron temperature; $I(k_z)$ is assumed to have only the Maxwellian part ; the slowing down part is neglected for simplicity. It is not so difficult to add the slowing part afterwards. $I(k_z)$ is shown in Fig. 1.

$I^0(k_z)$ is expressed by replacing $\Delta k_{x,y}$ with $\Delta\varphi_{x,y}$,

$$I^0(k_z)\Delta k_z = \phi \frac{k_z^3}{2\pi k_T^4} e^{-\frac{k_z^2}{k_T^2}} \cdot \Delta\varphi_x \Delta\varphi_y \Delta k_z = \phi \frac{k_z^3}{2\pi k_T^4} e^{-\frac{k_z^2}{k_T^2}} \cdot \left(\frac{\Delta Q_{min}}{\alpha k_z^{min}}\right)^2 \Delta k_z. \tag{14}$$

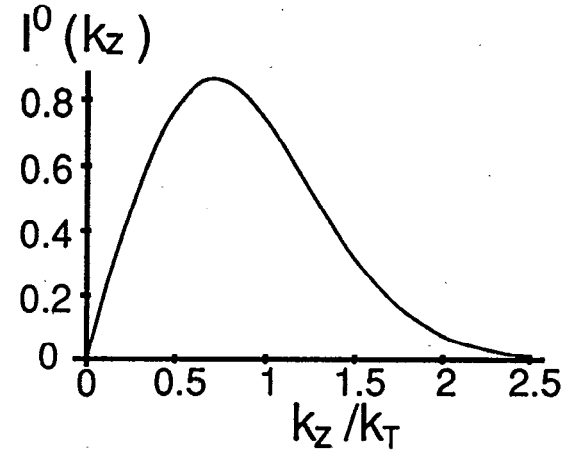

Fig. 1. Normalized spectrum, $I(k_z)$, at the sample position for a given $\Delta k_x \Delta k_y \Delta k_z$ resolution element. Only the Maxwellian part of the spectrum is shown as a function of k_z in units of k_T.

The importance of using a detector system with a large solid-angle is often overlooked in SANS instruments. The relation between solid-angle covered by a detector system and observed intensity is now discussed.

The solid angle subtended by a detector, $\Delta\Omega(\varphi)$, is expressed as

$$\Delta\Omega(\varphi) = 2\pi \sin\varphi\, \Delta\varphi = 4\pi \sin\frac{\varphi}{2} \cos\frac{\varphi}{2} \Delta\varphi, \tag{15}$$

where, φ is the scattering angle. Using the relations $Q = 2k_z \sin(\varphi/2)$ and $\Delta\Omega(k_z, Q)/\Delta Q$ for a fixed k_z is expressed as

$$\frac{\Delta\Omega(k_z, Q)}{\Delta Q} = \frac{2\pi Q}{k_z^2}, \quad (Q \le k_z). \tag{16}$$

$\Delta\Omega(k_z, Q)/\Delta Q$ is shown in Fig. 2. by a dashed line denoted by "Ideal".

F(Q) in eq. (10) can be expressed by using eqs. (12) and (15),

$$F(Q) = \int_{k_z^{min}}^{k_z^{max}} dk_z \frac{\phi k_z}{2\pi k_T^4} e^{-\frac{k_z^2}{k_T^2}} \Delta\varphi_x \Delta\varphi_y \, \eta(k_z, Q)\, Q$$

$$= \int_{k_z^{min}}^{k_z^{max}} dk_z \frac{\phi k_z}{2\pi k_T^4} e^{-\frac{k_z^2}{k_T^2}} \left(\frac{\Delta Q_{min}}{\alpha\, k_z^{min}}\right)^2 \eta(k_z, Q)\, Q. \quad (17)$$

Figure 3 gives the useful bandwidth in k_z for measurements at Q, which is determined by k_z^{min} and k_z^{max} in eq. (17) for both the reactor and pulsed source. The limits for $\Delta Q/Q = 0.1$ (long-dashed line) and $\Delta Q/Q = 0.3$ (short-dashed line) in the case of the pulsed source are shown in Fig. 3.

For the case of an instrument at a reactor, if $\Delta Q_{min}/Q_{min} = 0.1$ is required at Q_{min}, Δk_z becomes $0.1/\sqrt{3}\ k_z^{min} = 0.058\ k_z^{min}$. Therefore, integration over k_z should be taken from k_z^{min} to $k_z^{max} = k_z^{min} + \Delta k_z$ with $\Delta k_z = 0.058\ k_z^{min}$. A typical useful bandwidth in k_z is indicated by the short line with arrows outside in Fig. 3.

For the case of a pulsed source, integration can be carried out from k_z^{min} (or from cutoff at $Q=2k_z$), up to the line defined by $\Delta Q/Q = 0.1$. A typical integration path in the low-Q region is indicated by a thin horizontal arrow in Fig. 3.

Numerical integrations of eq. (17) for a pulsed source were performed and the Q dependences of F(Q) are shown in Fig. 4 for different values of k_z^{min} (= 0.2, 0.4, 0.6 and 1 $Å^{-1}$). Rapid drop of F(Q)'s beyond $Q = 2\ Å^{-1}$ is due to the fact that only the Maxwellian part of the spectrum was assumed for $I^0(k_z)$. If the slowing-down part of the spectrum is taken into account, F(Q)'s keep almost the peak values in a higher Q region.

The calculations were performed under the condition that $\Delta Q/Q \leq 0.1$, even at Q_{min} with $\Delta Q_{min} = 10^{-3}\ Å^{-1}$. Similar calculations for a reactor instrument for the same values of k_z^{min} are also shown by dashed straight lines in Fig. 4.

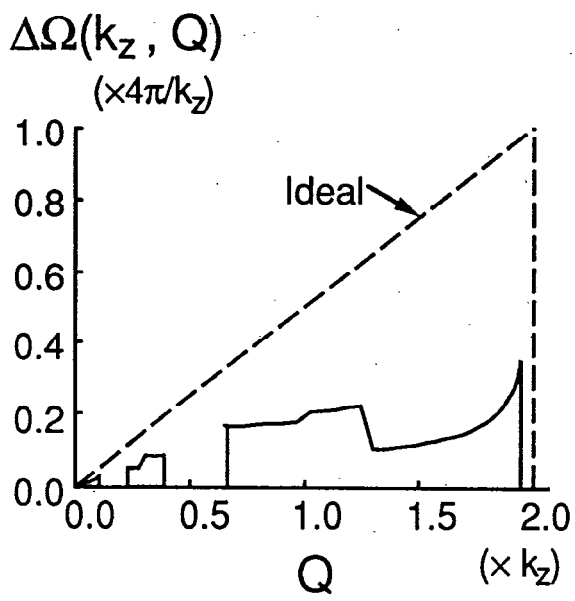

Fig. 2. $\Delta\Omega(k_z, Q)/\Delta Q$ as a function of Q for an ideal 4π solid-angle detector system for given kz (dashed line). The same function for WINK is also shown by thick solid curves.

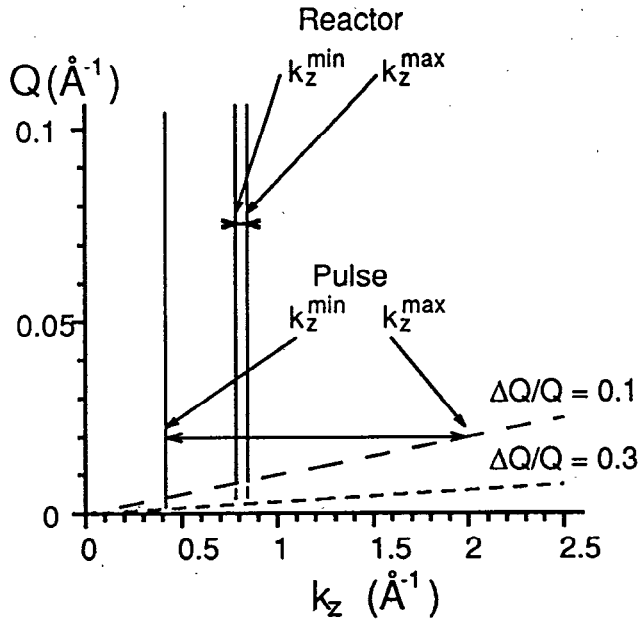

Fig. 3. Integration paths in a k_z-Q space.

In the case of a pulsed source, F(Q) increases drastically with decreasing k_z^{min}. This is because, a relaxed incident-collimation can be used with a smaller k_z^{min} to realize the same ΔQ_{min}. Under real experimental conditions, many difficulties arises when very small k_z is used: for example, a sample attenuation becomes serious at very small k_z and a measurement of transmission becomes difficult. A practical limit would lie around $k_z^{min} \approx 0.3\ Å^{-1}$ or $\lambda \approx 20$ Å.

In contrast, F(Q) for a reactor depends weakly on k_z^{min}. This is because, although $\Delta\varphi$ can be relaxed by using a smaller k_z^{min}, Δk_z should also be reduced as $\Delta k_z/k_z^{min} \approx 0.1$.

If only the first time-of-flight (TOF) frame is used, k_z^{min} for a pulsed source is expressed as

$$k_z^{min}\,(\text{Å}^{-1}) = \frac{2\pi}{3956}\cdot\frac{L\,(m)}{T\,(sec)}, \qquad (18)$$

where L is the total flight-path length and T the period of neutron bursts. In order to obtain a lower k_z^{min}, L should be as short as possible and T as long as possible over a realistic range. A smaller k_z^{min}'s can, of course, be realized by taking the second or third TOF frame, while sacrificing the bandwidth (smaller k_z^{max}); in general, though, this is not realistic. On the other hand, a smaller k_z^{min} can also be realized by thinning (reducing) the repetition of the neutron bursts while sacrificing ϕ. In this case, there is appreciable gain under certain conditions.

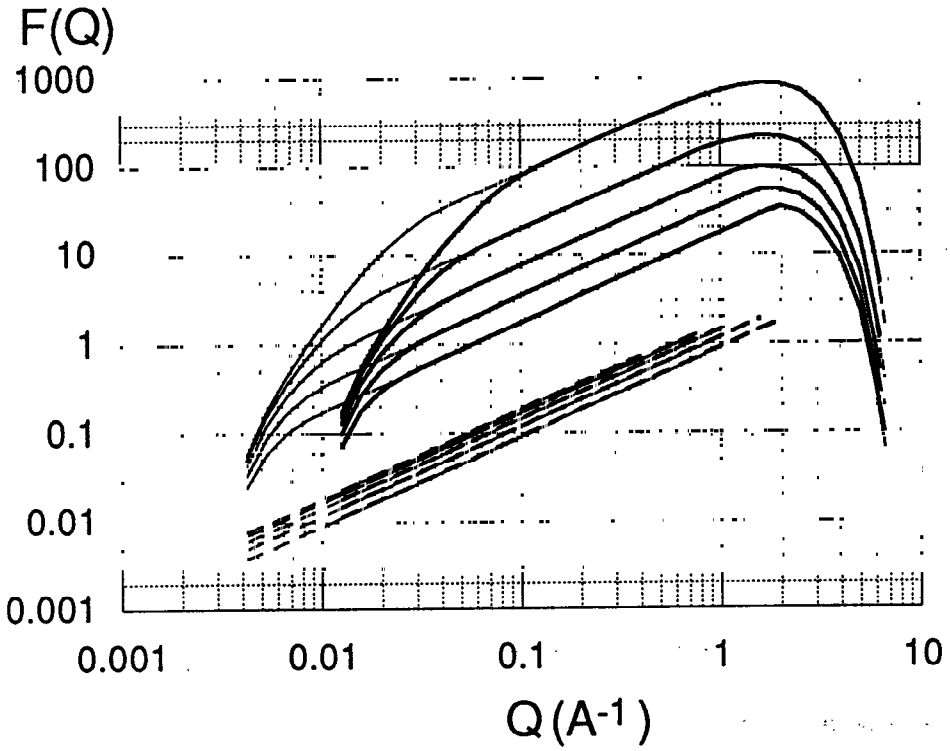

Fig. 4. Calculated F(Q) for k_z^{min} = 0.2, 0.4, 0.6, 0.8 and 1.0 Å^{-1}, from top to bottom for each type of plot. The solid curves are for a pulsed source with ΔQ_{min} = 0.001 Å^{-1}; $\Delta Q/Q \leq 0.1$ (thick lines) and ≤ 0.3 (thin lines), and dashed lines for a reactor source for $\Delta Q/Q \leq 0.1$ (thick lines) and for $\Delta Q/Q \leq 0.3$ (thin lines).

New small/medium-angle diffractometer WINK

As shown in the preceding sections, in constructing an ideal SANS instrument at a pulsed neutron source, the following conditions must be satisfied: i) period of neutron pulses as long as possible, ii) total flight path length as short as possible, and iii) detector solid angle as large as possible.

We designed and built a new small/medium-angle diffractometer, WINK, as shown in Fig.5, which satisfied the above conditions as much as possible. Unfortunately, there are many restrictions: for example, the beam line must be shared by three instruments! Actually, we built the WINK between two existing instruments: a low-energy inelastic spectrometer (LAM-40) and a high-resolution powder diffractometer (HRP). These three instruments share the same neutron beam (C4) viewing directly the solid methane moderator at 20K.

At KENS, the accelerator is operated at 20 Hz, which allows us a 50 msec bandwidth without reducing neutron pulses by a chopper. Since the total flight path-length is 11.3 m due to spatial limitations, k_z^{min} becomes 0.36 Å^{-1} (17.5 Å in wavelength). A tail-cutter is located at about 1.2 m upstream of the sample position, far from the moderator, for technical reasons. The frame overlap is, therefore, not negligible. We have a plan to install another tail-cutter just outside the biological shield. The sample position is 9 m from the moderator and the scattered flight-path-length is 2.3 m, which is much shorter than a desired length (about 4 to 5 m). We utilize a natural collimation between the moderator and the sample. The sample size was designed to be 20 mm by 20 mm. The detector arrangement at the small-angle position (L_2 = 2.3 m, φ = 1.5°~8.4°), which is installed inside the vacuum scattering chamber, is shown in Fig. 6. A similar detector arrangement is used at the

medium-angle position (L_2 = 1.1 m, φ = 12°~19°). The beam size of WINK is shown by a small square and the beam for HRP by a large rectangle, both shown in the center of the detector bank in Fig. 6. Conventional ^{3}He detectors of 1/2'-diameter are used at a lower-angle part, while at other angles 1'-diameter detectors are used. In order to squeeze as many detectors as possible into a compact space, detectors are slanted by 20 degrees, as shown in the figure. We have just installed them. Many high-angle detectors can be placed around the sample chamber, as shown in Fig. 5. The $\Delta\Omega(k_z, Q)/\Delta Q$ realized in WINK is shown by curves in Fig. 2. Even with the present detector arrangement, only 15-40% of the solid angle is covered, because of geometrical constraints.

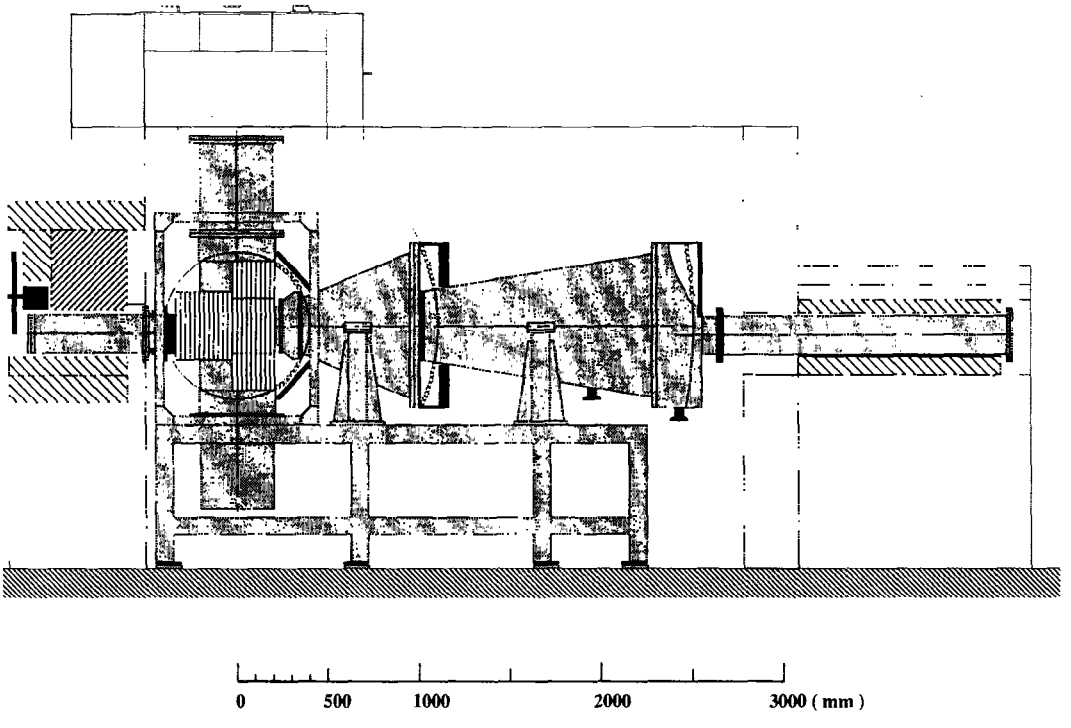

Fig. 5. Side view of WINK.

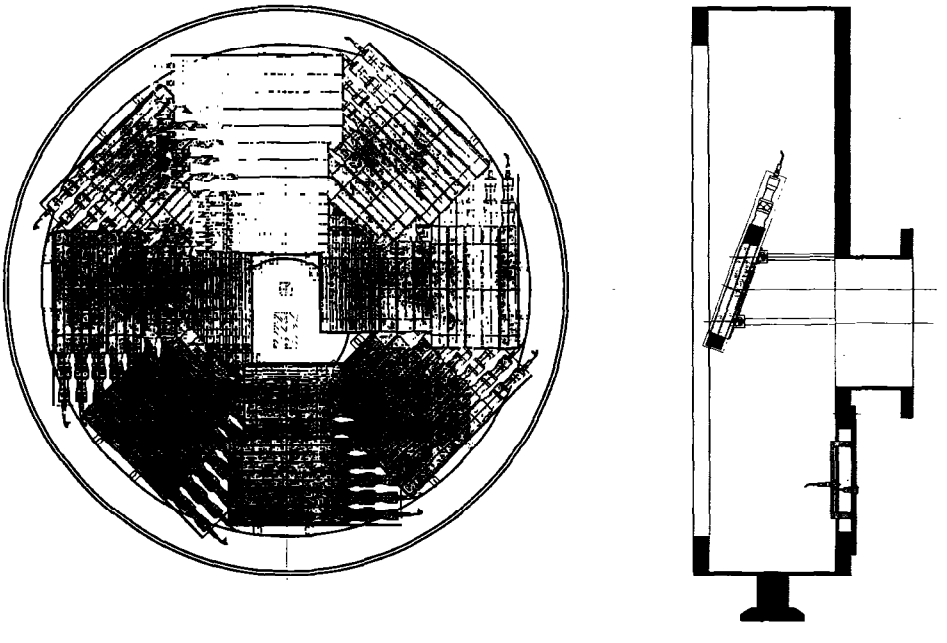

Fig. 6. Detector arrangement of a 2.3 m detector bank of WINK.

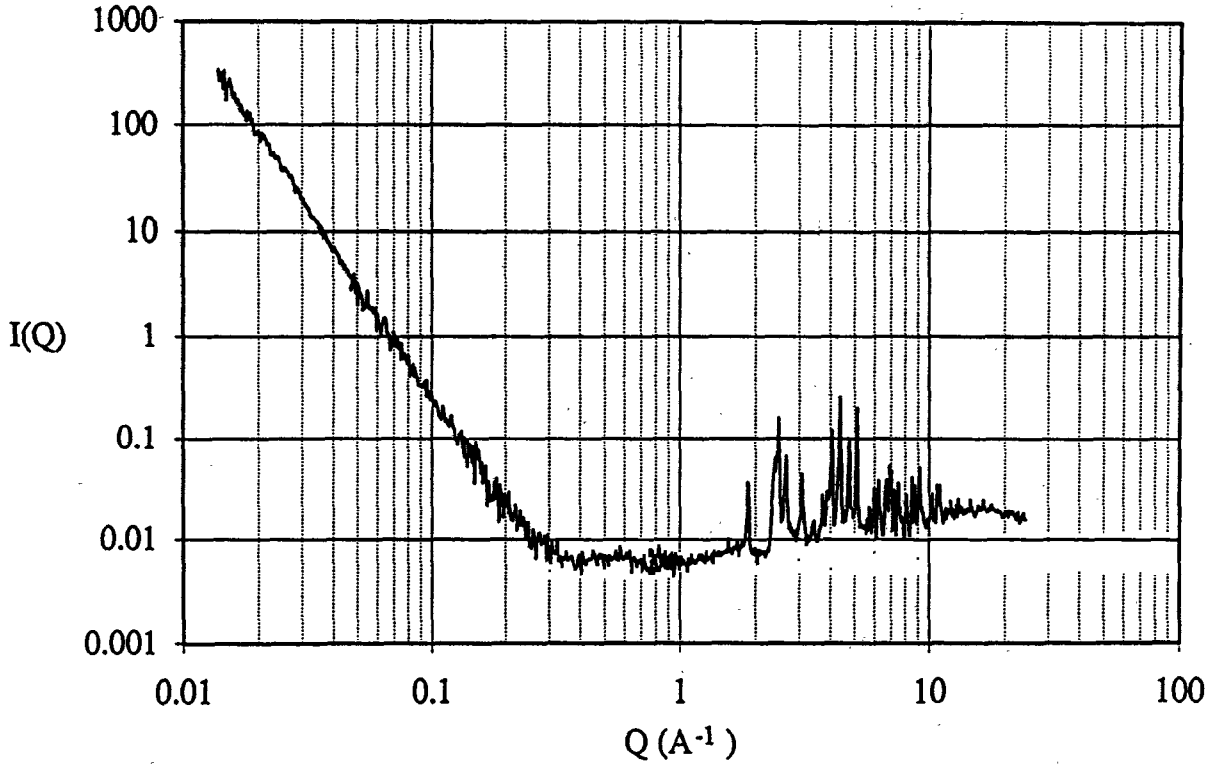

Fig. 7. Scattering spectrum from SiC fine powder measured by WINK instrument with only four detectors.

A preliminary scattering spectrum obtained from SiC fine powder using only one detector at each of four different scattering angles in about four hours is shown in Fig. 7. The Q-range covered by this instrument is sufficiently wide (Q = 0.015 - 20 Å^{-1}), as can be expected, and the dynamic range is almost 5 decades.

We are now constructing a high-angle detector bank as well as a sample changer. Only one fourth of the data-acquisition electronics is available now and a prototype data analysis software is under development. The instrument is expect to be completed within FY 1991.

Conclusions

From a total performance point of view, the utilization of neutrons with a wide k range, (especially that of small k_z^{min}), together with a detector system of a wide solid-angle coverage, plays essential roles in the case of a SANS instrument at a pulsed source.

WINK will be a hopefully ideal-like SANS instrument regarding the above points of view. However, there are many mismatches due to the various constraints: narrow space, beam shared with two other instruments, and so on.

References

Maier-Leibnitz H., Nukleonik **8** (1966) 61.

Alefeld B. and Kollmar A., Proc ICANS-VIII (1985) 385, (Rutherford Appleton Laboratory Report RAL-85-110, 1985).

Q(A. D. Taylor): How does the resolution change with angle impact on the data analysis?

A(M. Furusaka): The higher is the scattering angle, the better is the relative resolution $\Delta Q/Q$ owing to the $\cot(\varphi/2)$ term. Only data from the small-angle part affect the analyzed scattering function.